# Human/robotic interaction: Vision limits performance in simulated vitreoretinal surgery

**Short Title**: Vision effect on accuracy and precision in VR robotics

Marc D. de Smet[1,2]

Nicky de Jonge [2]

Danilo Iannetta [3]

Koorosh Faridpooya [4]

Eric van Oosterhout [5]

Gerrit Naus [2]

Thijs CM Meenink [2]

Marco Mura [6]

Maarten J Beelen [2]

[1] Microinvasive Ocular Surgery Center (MIOS sa) Lausanne, Switzerland

[2] Preceyes BV, Eindhoven, the Netherlands

[3] Royal Liverpool University Hospital, St Paul's Eye Unit, United Kingdom; University of Tor Vergata, Dept of Clinical Sciences and Translational Medicine, Rome, Italy

[4] Rotterdam Eye Hospital, Rotterdam, the Netherlands

[5] Catherina Ziekenhuis, Eindhoven, the Netherlands

[6] Faculty of Medicine, Johns Hopkins University, Baltimore, United States; King Khaled Specialist Eye Hospital, Riyadh, Saudi Arabia

Reprint requests and correspondence: Marc D. de Smet; Av du Léman 32, Lausanne 1005, Switzerland. tel.: +41-21-566-1222, fax: +41-21-566-1865; E-mail: mddesmet1@mac.com

**Abstract:**

**Purpose:**

Compare accuracy and precision in XYZ of stationary and dynamic tasks performed by surgeons with and without the use of a tele-operated robotic micromanipulator in a simulated vitreoretinal environment. The tasks were performed using a surgical microscope or while observing a video monitor.

**Method:**

Two experienced and two novice surgeons performed tracking and static tasks at a fixed depth with handheld instruments on a Preceyes Surgical System R0.4. Visualization was through a standard microscope or a video display. The distances between the instrument tip and the targets (in µm) determined tracking errors in accuracy and precision.

**Results:**

Using a microscope, dynamic or static accuracy and precision in XY (planar) movements are similar among test subjects. In Z (depth) movements, experience lead to more precision in both dynamic and static tasks (dynamic 35 ± 14 vs 60 ± 37 µm; static 27 ± 8 vs 36 ± 10 µm), and more accuracy in dynamic tasks (58 ± 35 vs 109 ± 79 µm). Robotic assistance improved both precision and accuracy in Z (1 to 3 ± 1 µm) in both groups. Using a video screen in combination with robotic assistance improved all performance measurements and reduced any differences due to experience.

**Conclusions:**

Robotics increases precision and accuracy, with greater benefit observed in less experienced surgeons. However, human control was a limiting factor in the achieved improvement. A major limitation was visualization of the target surface, in particular in depth. To maximize the benefit of robotic assistance, visualization must be optimized.

**Key Words:**

Robotics; telemanipulation; simulation; vitreoretinal surgery; depth perception; accuracy; precision

**Introduction:**

Success in surgery depends on a number of factors: a surgeon's skill, the ability to adequately visualize the surgical field, the availability of adequate and adapted surgical instrumentation (Reznick et al. 1996; Lyons et al. 2013; Yadav et al. 2016). Experience is what allows a surgeon to reliably carry out surgical tasks with precision and accuracy under a constantly changing visual environment.

When evaluating the surgical field, and judging the extent and nature of motion, visual perception is the major source of information at a surgeon's disposal. During VR surgery, the surgeon sees the operating scene through a binocular microscope or a heads-up display. This provides him with a three dimensional representation of the surgical space, allowing him to estimate distances between instruments and target structures. While under optimal conditions, a 10μm visual resolution can be achieved in XY (the planar field), much lower resolutions are observed when visualisation is poor due to media opacities. In the Z axis, where depth perception is important, observed resolutions are much lower under all conditions. Static tasks as compared to dynamic tasks present additional physiological challenges. Human hand motion has certain inherent limitations, including physiologic tremor, jerks and low frequency drift (Riviere et al. 1997). All of these are accentuated when attempting to remain stationary or when actuating an instrument (Riviere et al. 1997). Robotic assistance can improve dexterity, accuracy, and precision, and has been introduced to a number of surgical procedures (Noda et al. 2013). Its ability to stabilize and improve the accuracy of surgical task in ophthalmic surgery has also been extensively investigated with a hand held tool called the steady hand (Taylor et al. 1999; Maclachlan et al. 2012; Gonenc et al. 2014). Other approaches that are being developed for ophthalmic applications include robotic systems that make use of telemanipulation, comanipulation or intraocular nanoparticles (de Smet et al. 2018).

In this article, we concentrate on demonstrating the accuracy and precision of a telemanipulation system. The terms precision and accuracy are often used interchangeably. From a surgical standpoint, accuracy refers to the proximity achieved in reference to an intended target, while precision refers to the degree of reproducibility of the motion or procedure (Zrinzo 2012). Accuracy is frequently the only parameter that is investigated. In this article, we have attempted to measure both, where accuracy refers to the position of an instrument's tip with respect to the target's position, while precision refers to how close repeated measurements are to each other. Accuracy and precision were measured for all three cardinal positions XYZ, evaluating the performance of manual versus robot assisted tasks in experienced and novice test subjects. In the process, the limitations of visual perception as a quantitative parameter on manual performance in both sets of subjects was observed noting differences between planar XY and depth Z tasks. Depth tasks are particularly dependent on experience. Here, robotic assistance provided by a telemanipulator can be of particular help in accelerating a surgeon's ability to perform complex tasks.

**Materials & methods**

For the purpose of these experiments, a prototype robotic telemanipulator developed by Preceyes BV (Eindhoven, the Netherlands) was used (Meenink et al. 2012; de Smet et al. 2016). The prototype used in these experiments was a preclinical version labelled R0.4. This robotic-assistant functions as a tele-operated micromanipulator. A motion-controller activated by the surgeon provides input to a computer which drives an instrument-manipulator to which are attached intraocular instruments. The Preceyes robot modifies its scaling as an instrument or device penetrates deeper into the eye. The experiments were carried out at a fixed depth, simulating surgery in the macular region. Both static and dynamic accuracy were measured, where static accuracy refers to the ability to maintain a fixed position during a specified time period, and dynamic accuracy is that which is achieved during active motion between two points within a three-dimensional space. Each experiment was carried out with or without the assistance of the micromanipulator. For manual, unassisted procedures, the instrument was held in the surgeon's hand with appropriate unobtrusive support of his forearm (figure 1.1).

Alternatively, the micromanipulator held the instrument while the motion was initiated using the motion controller held in the surgeon's hand (figure 1.2). Initial tests were carried out while looking through an ophthalmic microscope. The same experiments were later repeated while looking at a computer screen away from the surgical field (figures 1.4 and 1.5). A comparison of the accuracy and precision with and without assistance allowed an assessment of the value of robotic assistance, while microscopic viewing versus observation of a video monitor enabled an assessment of the influence of the visual modality on performance. Dynamic and static accuracy were tested on 4 test subjects, 2 of which were senior VR surgeons. Each test subject was allowed to familiarize himself with the robotic system by performing several surgical simulations designed to teach the surgeon how to work with the system**.** They were also allowed to familiarize themselves with the experimental set-up. Once the test subjects felt comfortable performing the required tasks, the experiment was carried out, acquiring for each person 3 datasets. Between each repeat, a rest period was allowed to prevent fatigue.

For the purpose of the analysis, position measurements were deducted from the images obtained from the cameras and recorded as µm. The distances between the instrument tip and the target were measured as tracking errors. The absolute tracking errors were used as an accuracy measure, the standard deviation of all tracking errors was used as a precision measure. An average tracking error for accuracy and precision, standard deviation for both and maximum accuracy error were determined. For the maximum measurement the absolute maximum value of all tests was taken.

**Simulated surgical setup, and test procedure:**

A model eye was designed to simulate a vitreoretinal environment (figure 2). Prior to its use in the experiments described below, measurements obtained from manual surgical simulations were validated against existing published data. The model consisted of a styrofoam base to which was fitted a modified silicone model eye (VR Eyelab Innovation - Oregon, USA). Inside the sphere a 1 cm x 1 cm piece of checkered graph paper (square length of 1 mm) was positioned centrally. This was used as a target for the first set of experiments. At its apex, the artificial sclera had an opening corresponding to the diameter of the cornea (10 mm), enabling visualization through an ophthalmic microscope (OPMIcs on an S4 floor stand, Carl Zeiss, Jena, Germany). To fully simulate a vitreoretinal surgical setting, the microscope was fitted with a BIOM V, an inverter and a 90 D lens (Oculus Surgical Inc, Port St Lucie, Fl, USA). Four millimetres posterior to the edge of this opening, a 23G trocar was inserted to allow passage of instruments into the sphere (figure 3).

A video camera (Handycam HDR-CX240, 9.2 MegaPixels, Sony Corp, Japan) was mounted to the microscope which recorded the XY movements of the instrument tip. The recordings were captured at 50 frames/sec, and the pixel distances between the instrument tip and the target points were measured as tracking errors. To record in the Z direction, an opening was made in the styrofoam base to allow lateral view of the lower portion of the eye model. An identical camera was positioned horizontally focused on the needle tip. Magnification was held constant, but the focus adjusted prior to an experimental run (figure 4).

In each experimental run, test subjects were asked to position the tip of the test instrument above the edge of an inner square of the grid (figure 5). Each test subject was instructed to maintain the height above the grid as constant as possible while tracing and while holding the instrument motionless. When in position, test subjects were instructed to follow as accurately as possible, irrespective of time, the line corresponding to the outer edge of 4 grid squares (2 mm by 2 mm).When reaching the edge of the square, the test subject was asked to hold the tip motionless at that position for 30 seconds. He was then instructed to continue along the line to the following corner. To determine accuracy and precision in the z-direction, the surgeon was asked to carry out these tasks at a fixed height above the grid. These tests were carried out with and without robotic assistance (figure 1.1, 1.2).

**Motion measurements using a laser vibrometer**

In these experiments, only the upper portion of the model eye was retained and fixed to a hollow styrofoam cylindrical base, open on one side (figure 6). The instrument tip was inserted in the eye model, and the tip fitted with a flat reflective surface. A laser vibrometer OVF-5000 (Polytec GmbH, Waldbronn, Germany) containing a fiber optic sensor head (OVF-552) was used to generate a laser beam directed onto the instrument tip's reflective surface. The detected signal was analyzed using a displacement decoder (DD-500, Polytec GmbH) set at 500µm/V, which provides a unidirectional position measurement. The test set-ups are summarized in figures1.3 and 1.6.

The test subjects were asked to look at a 24 inch video screen positioned 0.5 m in front of them at eye height. The screen projected a magnified image corresponding to a 2 mm interval located around the tip of the laser. The screen projected two lines: a target line which was either fixed (static test) or moving at a rate of 0.02 mm/s (dynamic test), and a second line corresponding to the instrument tip. The test subject was asked to overlay the instrument line over the target line for the duration of each test sequence. The position in all three directions (XYZ) were measured independently (figure 7). During the dynamic exam, the target line was projected for 100 seconds (equivalent to a 2 mm distance), while in the static test, the subject was asked to maintain the overlay for 30 seconds. The positions of both the instrument and the target were logged at 100 Hz, and the distances between the instrument position and the target were measured as tracking errors. The experiments were carried out with and without the assistance of the tele-operated micromanipulator (figures 1.4 and 1.5).

**Evaluation of the precision of the micromanipulator's subsystems**

To test the inherent accuracy and precision of the robotic micromanipulator and its subsystems, the vibrometer setup was used. First a subsystem was created in which the manipulator was programmed to automatically trace the target in a dynamic test. Using the output of the laser vibrometer as a position measurement, the robot was controlled automatically (figure 1.3). An automated computer routine was initiated in which the instrument tip was required to automatically follow a programmed movement, while the motion of the tip was recorded using the laser vibrometer.

To evaluate the motion controller as a separate subsystem, a virtual-reality set-up was created in which the motion controller was operated by the test subjects as previously described, except that the instrument manipulator was simulated, generating virtual positional information at the tip of the instrument (figure 1.6).

**Results:**

We first report the results obtained with the robot operating in an automated mode. These results for the instrument manipulator are reported in table 1. These results can be interpreted as the inherent accuracy and precision of the instrument manipulator as a separate subsystem. Both precision and accuracy are in the µm range. The observed maximum accuracy errors result from disturbances from neighbouring mechanical equipment.

Table 2 provides the accuracy and precision results for set-up 1.6 in which the motion controller is evaluated. The results show that the motion controller's static accuracy is similar to the measurements observed with the instrument manipulator in table 1.

In the experiments requiring test subjects, we made use of 2 experienced surgeons in their early 50's with more than 15 years of experience in vitreoretinal surgery and 2 younger subjects 20 years younger. In table 3, we report the dynamic and static accuracies achieved, performing manual tasks while using the microscope. In static tasks, accuracy and precision were similar between experienced and less experienced individuals. However, in dynamic tasks, experience leads to a more accurate and precise positioning in the Z direction in dynamic tasks.

Robotic assistance improved a surgeon's performance for both precision and accuracy and is reported in table 4. The results in both experienced and inexperience test subjects were similar. Automated robotic procedures were 7.5 and 87 fold better in accuracy and precision than manually performed tasks. Static tasks in Z were similar to the performance levels of the instrument manipulator on its own, while XY accuracy was lower possibly due to human override. The latter is likely also the source of the observed difference between table 1 and 4 in the dynamic mode.

The test results using the laser vibrometer are provided in table 5. In this set-up, the effect of the microscope on precision and accuracy is evaluated. In static tests, the assisted mode in both horizontal and vertical directions was comparable in precision and accuracy to the level achieved by the robot independent of human interaction. Unassisted static accuracy was high but with a significantly higher maximum accuracy error (17X to 104X). Dynamic accuracy was similar to static accuracy when the task was robotically assisted. It was less accurate by a factor of 1.4x to 8.5x when unassisted. However, the values were in all cases 5x or more lower with the test subject looking at a computer screen rather than through the microscope (Tables 3&4 vs 5). Dynamic precision levels remained similar in both assisted and unassisted modes whether or not the target was visualized through a microscope or simulated on a computer screen.

**Discussion:**

The current study measured the dynamic and static accuracy and precision of a robotic tele-operated micromanipulator designed for ocular surgery. The set-up enabled testing of both parameters in a simulation that closely approximated a surgical environment. In preliminary experiments, we tested the validity of our set-up against reported data for free-hand movement. Then, we measured the inherent accuracy and precision of the micromanipulator arm in all three primary positions at between 1-3µm. The sensitivity of the set-up was such that it was able to pick up noise from the environment, similar to the vibration previously described by Nakano et al (Nakano et al. 2009). These experiments allowed us to show that robotic assistance improved performance of all test subjects, but subjects with minimal experience benefited most.

Previous positional stability tests of a simulated instrument held by ophthalmic surgeons showed that the maximum drift was about 350 µm, while in dynamic testing, accuracy decreased depending on the speed of motion to values between 2000 and 7000 µm (Riviere et al. 1997; Peral-Gutierrez et al. 2004). Both in dynamic and static tasks, free hand gestures were influenced by inherent involuntary human physiological factors such as tremor, jerks, and low frequency drift, which limitws the physiologic reach of both parameters(Riviere et al. 1997; Riviere et al. 2006). Similar pointing and tracing tests have been carried out in other robotic experiments. Nakano et al. tested experienced surgeons of various levels (7 to 20 years) using a target structure of 1x1 mm (Nakano et al. 2009). Dynamic accuracy, static accuracy and the maximum static accuracy error, were measured in a horizontal plane. Surgeons were required to visualize the test plane through a 3D video screen. They achieved a static accuracy of approximately 70 µm, an average dynamic accuracy of approximately 58 µm and a maximum static accuracy error of approximately 330 µm, ranges which are similar to our own measurements. Interestingly, in their set-up, they did not observe any difference in accuracy based on experience, ascribing the differences to variations in physiologic tremor. Our research showed that the accuracy errors achieved when robotic assistance was used were lower than when the test subjects were unassisted. These findings are also supported by the literature (Nakano et al. 2009; Noda et al. 2013). Nakano in his experimental set up reported measurements that were significantly improved with appropriate dampening of tremor. Noda et al, using a different master-slave set-up showed that the aiming accuracy and positional stability of ophthalmologists was superior to that of engineering students, but while robotics improved significantly the positional stability of both groups, it had little effect on aiming accuracy of ophthalmologists in a dynamic task (Noda et al. 2013). In the XY plane, we obtained similar results. Both experienced and inexperienced test subjects were able to achieve quite acceptable and comparable levels of accuracy both statically and dynamically. However, in the Z axis, experience lead to greater dynamic accuracy. In all test conditions, the use of robotic assistance lead to improvement in test results and eliminated the difference between the two groups.

While we demonstrated an inherent accuracy and precision of the instrument-manipulator subsystem of 1-3µm, this accuracy and precision is an order of magnitude better than when the tasks were carried out by test subjects. Hence, here lies a challenge in fully exploiting the potential benefits of robotic assistance. Our research indicates that the difference is likely linked, at least in part, to the limitations placed by the visualization system used by the surgeon and to the judgements calls he makes to execute his surgical tasks.

Judging position in the vertical axis is a crucial task in ophthalmic surgery, and is dependent as much on monocular cues as on depth perception through the microscope. In a prospective study, Gizicki analyzed video recordings of internal limiting membrane peels by vitreoretinal fellows and accomplished vitreoretinal surgeons with 10 or more years of experience (Gizicki et al. 2017). The number of flap initiation attempts was significantly higher in surgeries performed by fellows, as was the number of retinal/RPE contusions, and peel-related hemorrhages, though these differences did not reach statistical significance. In a virtual environment, some of the most prominent faults were reported as spotted hemorrhages, injury to the macula or peripheral retina, and vessel hits by laser, all of which indicate some difficulty with depth perception (Deuchler et al. 2016). Lower complication rates were seen with more experience. An inverse correlation between stereopsis and the number of retinal contacts per average time was also noted in another simulation experiment, where a generated “stereopsis score” was in direct correlation with experience (Rossi et al. 2004).

Depth perception is not directly related to stereopsis. Much of our perception of depth may be related to motion in depth, itself dependent on interocular velocity differences and perceived changes in disparity over time (Harris et al. 2008). Furthermore, horizontal pointing experiments reveal that movements are planned using either a hand - or target-center frame of reference (Vindras et al. 2005). Visualization through a microscope makes use of the latter and requires the acquisition of specific skills. Indeed experienced and inexperienced surgeons do not seem to differ in their pointing accuracy in free space or when using a navigational monitor, but experience plays a significant role when performing the same task through a microscope (Hirata et al. 1998). The difference are attributable to poorer depth perception of phantom surgical spaces by inexperienced surgeons. Depth perception through a microscope limits a surgeon's ability to perform precision tasks. This limitation is reflected in the observed dynamic accuracies using robotic assistance through a microscope (table 4). The use of a video monitor as in our vibrometer tests, improved the performance of both dynamic and static parameters (table 5) in both the assisted and unassisted modes, and for both horizontal and vertical tasks. In this setting, the differences related to experience are much less visible.

Our research indicates that to maximize the potential of robotic assistance, novel strategies will have to be implemented either by improving visualization of the surgical field, using enhanced positing strategies, or by making use of machine vision. A surgeon's use of heads-up displays can improve his depth perception (Eckardt &  Paulo 2016), while the intraoperative OCT can improve his ability to position robotic instruments within the eye (Ehlers et al. 2015; Siebelmann et al. 2016). Such means will improve upon existing static tasks, but may be more difficult to apply to a moving target. By incorporating feedback directly into the robot, through the use of a closed loop position control, both dynamic and static tasks can be improved (Bouget et al. 2017). This introduces the need for real-time intraocular distance measurements - either through external precision monitors or by enhanced instrumentation.

**References:**

Bouget D, M Allan, D Stoyanov & P Jannin (2017): Vision-based and marker-less surgical tool detection and tracking: a review of the literature. Med Image Anal 35: 633-654.

de Smet MD, TC Meenink, T Janssens, V Vanheukelom, GJ Naus, MJ Beelen, C Meers, B Jonckx & JM Stassen (2016): Robotic Assisted Cannulation of Occluded Retinal Veins. PLoS One 11: e0162037.

de Smet MD, GJL Naus, K Faridpooya & M Mura (2018): Robotic-assisted surgery in ophthalmology. Curr Opin Ophthalmol 29: 248-253.

Deuchler S, C Wagner, P Singh, M Muller, R Al-Dwairi, R Benjilali, M Schill, H Ackermann, D Bon, T Kohnen, B Schoene, M Koss & F Koch (2016): Clinical Efficacy of Simulated Vitreoretinal Surgery to Prepare Surgeons for the Upcoming Intervention in the Operating Room. PLoS One 11: e0150690.

Eckardt C & EB Paulo (2016): Heads-up surgery for vitreoretinal procedures: An Experimental and Clinical Study. Retina 36: 137-147.

Ehlers JP, J Goshe, WJ Dupps, PK Kaiser, RP Singh, R Gans, J Eisengart & SK Srivastava (2015): Determination of feasibility and utility of microscope-integrated optical coherence tomography during ophthalmic surgery: the DISCOVER Study RESCAN Results. JAMA Ophthalmol 133: 1124-1132.

Gizicki R, D Chow, MYK Mak, DT Wong, RH Muni, F Altomare, AR Berger & LR Giavedoni (2017): Differences in surgical performance of internal limiting membrane peeling for macular hole repair between supervised vitreoretinal fellows and vitreoretinal faculty at a single institution. J VitRet D 1: 305-309.

Gonenc B, E Feldman, P Gehlbach, J Handa, RH Taylor & I Iordachita (2014): Towards Robot-Assisted Vitreoretinal Surgery: Force-Sensing Micro-Forceps Integrated with a Handheld Micromanipulator. IEEE International Conference on Robotics and Automation : ICRA : [proceedings] IEEE International Conference on Robotics and Automation 2014: 1399-1404.

Harris JM, HT Nefs & CE Grafton (2008): Binocular vision and motion-in-depth. Spatial Vis 21: 531-547.

Hirata M, A Kato, T Yoshimine, S Nakajima, M Maruno, S Tamura, F Kishino & T Hayakawa (1998): Spatial perception in macroscopic and microscopic surgical manipulations: differences between experienced and inexperienced surgeons. Neurol Res 20: 509-512.

Lyons C, D Goldfarb, SL Jones, N Badhiwala, B Miles, R Link & BJ Dunkin (2013): Which skills really matter? proving face, content, and construct validity for a commercial robotic simulator. Surg Endoscopy 27: 2020-2030.

Maclachlan RA, BC Becker, JC Tabares, GW Podnar, LA Lobes, Jr. & CN Riviere (2012): Micron: an Actively Stabilized Handheld Tool for Microsurgery. IEEE Trans Robot 28: 195-212.

Meenink HCM, R Hendrix, MJ Beelen, GJL Naus, EJGM van Oosterhout, MD de Smet, PCJN Rosielle, H Nijmejier & M Steinbuch (2012): Robot-assisted vitreoretinal surgery In: Gomes P(ed.) Surgical Robotics Part II - Applications. London. Woodhead Publishing.

Nakano T, N Sugita, T Ueta, Y Tamaki & M Mitsuishi (2009): A parallel robot to assist vitreoretinal surgery. Int J Comp Assist RadiolSurg 4: 517-526.

Noda Y, Y Ida, S Tanaka, T Toyama, MF Roggia, Y Tamaki, N Sugita, M Mitsuishi & T Ueta (2013): Impact of robotic assistance on precision of vitreoretinal surgical procedures. Plos One 8: e54116.

Peral-Gutierrez F, AL Liao & CN Riviere (2004): Static and dynamic accuracy of vitreoretinal surgeons IEEE EMBS. San Francisco. IEEE: 2734-2737.

Reznick R, G Regehr, H MacRae, J Martin & W McCulloch (1996): Testing technical skill via innovative “bench station” examination. Am J Surg 172: 226-230.

Riviere CN, J Gangloff &  M de Mathelin (2006): Robotic compensation of biological motion to enhance surgical accuracy. Proc IEEE 94: 1705-2716.

Riviere CN, RS Rader &  PK Khosla (1997): Characteristics of hand motion of eye surgeons 19th Annual Conference of the IEEE Engineering in Medicine and Biology Society. Chicago, USA. IEEE.

Riviere CN, RS Rader &  PK Khosla (1997): Characteristics of hand motion of eye surgeons IEEE Engineering in Medicine and Biology Society. Chicago.

Rossi JV, D Verma, GY Fujii, RR Lakhanpal, S Lynn, MS Humayun &  E de Juan, Jr (2004): Virtual vitreoretinal surgical simulator as a training tool. Retina 24: 231-236.

Siebelmann S, C Cursiefen, A Lappas &  T Dietlein (2016): Intraoperative Optical Coherence Tomography Enables Noncontact Imaging During Canaloplasty. J Glauc 25: 236-238.

Taylor R, PE Jensen, L Whitcomb, AC Barnes, R Kumar, D Stoianovici, P Gupta, ZX Wang, E De Juan &  L Kavoussi (1999): A steady-hand robotic system for microsurgical augmentation. Int J Robot Res 18: 1201-1210.

Vindras P, M Desmurget &  P Viviani (2005): Error parsing in visuomotor pointing reveals independent processing of amplitude and direction. J Neurophysiol 94: 1212-1224.

Yadav YR, V Parihar, S Ratre, Y Kher &  M Iqbal (2016): Microneurosurgical Skills Training. Journal of neurological surgery. Part A, Cent Eur Neurosurg 77: 146-154.

Zrinzo L (2012): Pitfalls in precision stereotactic surgery. Surg Neurol Intern 3: S53-61.

Figure Legends:

**Figure 1: Schematic showing the experimental set-ups used to test both manual and robotic assisted surgical simulations.**

Surgeons were asked to look at the target through a surgical microscope or on a video monitor.

**Figure 2: Lateral view of the eye model and grid target used during the testing procedure.**

The instrument was inserted into the mould through the trocar, and the test subject was asked to follow appropriate instructions as described in the methodology section.

Figure 3: Vertical camera shot showing the position of t**he robotic arm in relation to the BIOM.**

The vertical camera shot is taken through a side arm of the surgical microscope and corresponds to the image seen by the surgeon.

Figure 4: **The horizontal camera view.**

With a fixed magnification, the distance between the instrument tip and the surface plane of the grid was measured in μm.

Figure 5: **Schematic showing the position of the camera**

In relation to the tip of the instrument, including an image of the target from which the tracking error was measured in experiments carried out using the microscope.

Figure 6: **Set-up for the laser vibrometer and videoscreen.**

The left image shows the vibrometer and instrument set-up. In the right image is a simulation of the monitor observed by the test subject. He is instructed to superimpose or maintain the red line (indicating the position of the probe tip) over the fixed blue line. The screen being observed is visible in the background of the image on the left.

Figure 7: **Schematic representation of the test set-up using the vibrometer indicating the direction of the measurement.**

The blue arrows indicate the direction of motion of the instrument and the red laser point indicates how the laser is directed towards the instrument tip.

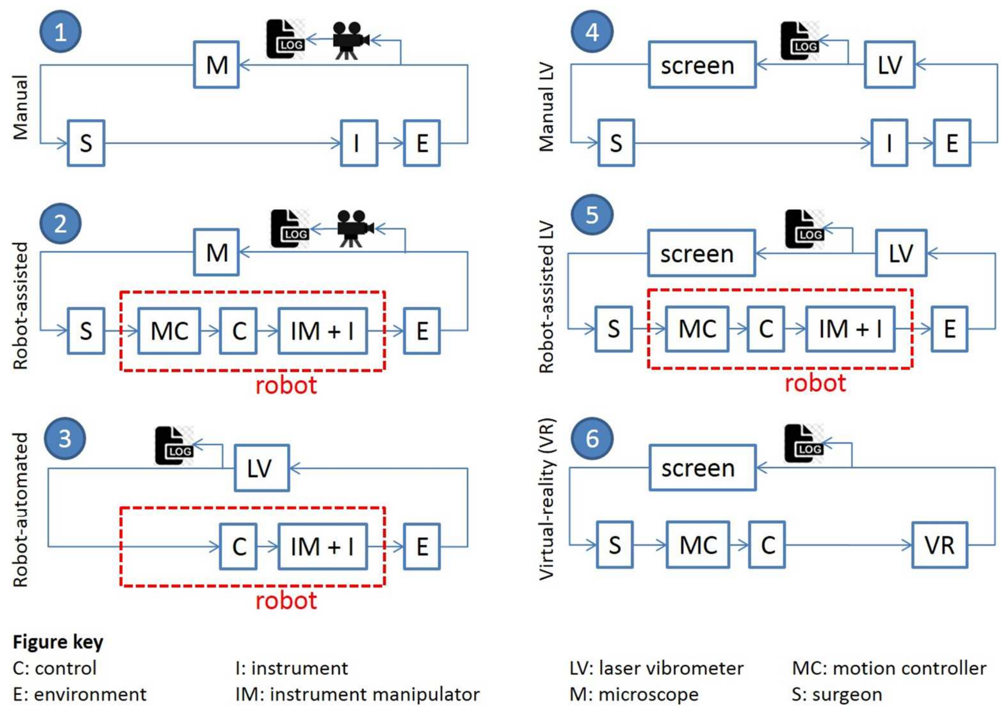


Schematic showing the experimental set-ups used to test both manual and robotic assisted surgical simulations using the microscope or the video monitor

114x81mm (300 x 300 DPI)

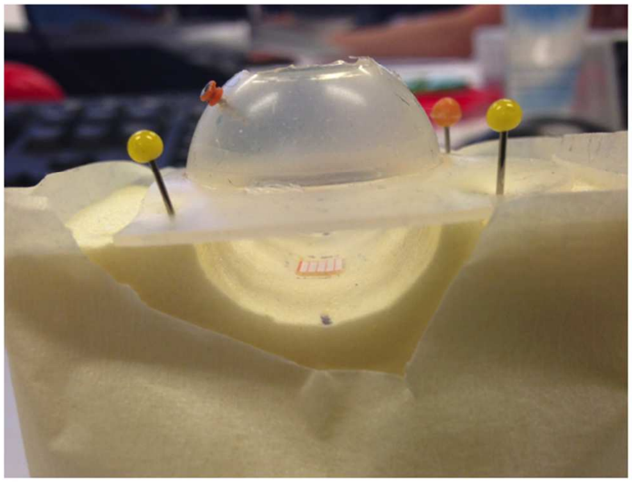

Lateral view of the eye model and grid target used during the testing procedure

86x65mm (300 x 300 DPI)

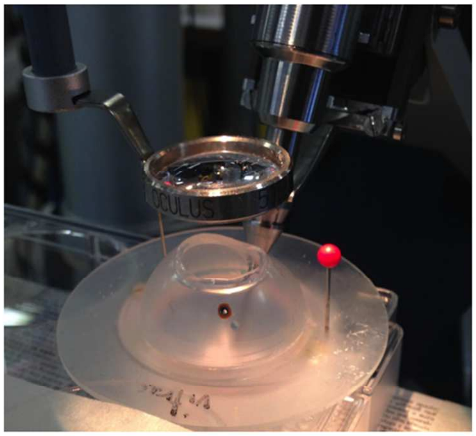


Vertical camera shot showing the position of the robotic arm in relation to the BIOM.

86x65mm (300 x 300 DPI)

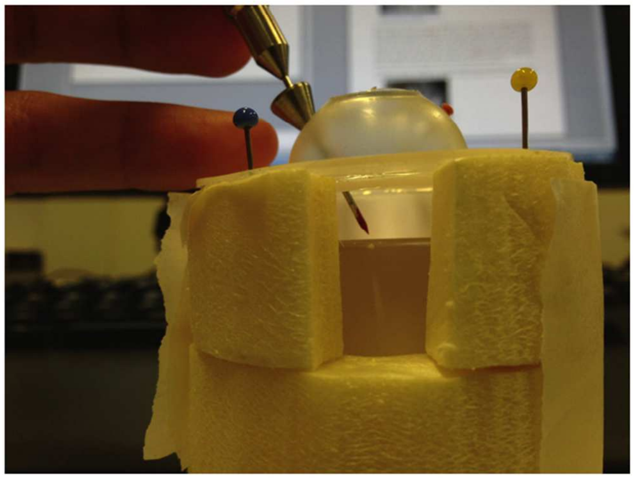

Horizontal camera view. A fixed magnification allows a measurement of distance between the instrument tip and the grid in μm.

86x65mm (300 x 300 DPI)

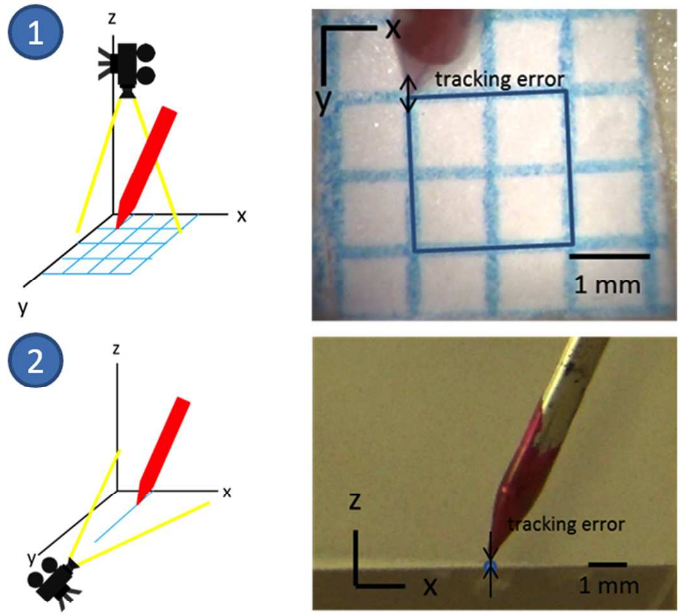


Schematic showing the position of the camera related to the tip of the instrument, including an image of the target from which the tracking error was measured in experiments carried out using the microscope

86x65mm (300 x 300 DPI)

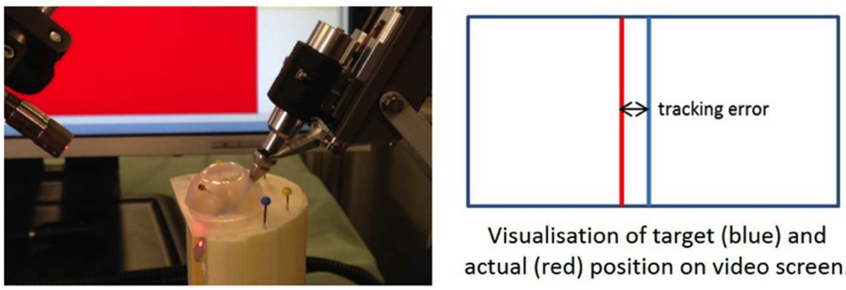


Set-up for the laser vibrometer and video screen. The left image shows the vibrometer and instrument set-up. In the right image is a simulation of the monitor observed by the test subject. He is instructed to superimpose or maintain the red line (indicating the position of the probe tip) over the fixed blue line. The screen being observed is visible in the background of the image on the left.

86x65mm (300 x 300 DPI)

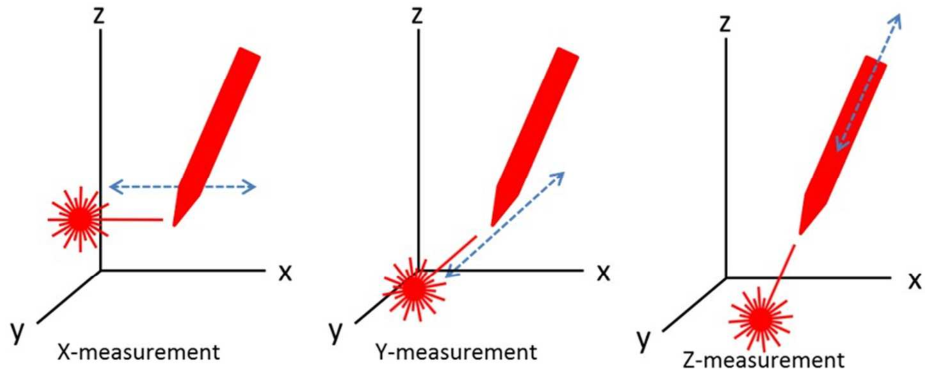


Schematic representation of the test set-up using the vibrometer indicating the direction of the measurement. The blue arrows indicate the direction of motion of the instrument and the red laser point indicates how the laser is directed towards the instrument tip.

82x32mm (300 x 300 DPI)

Table 1: Average tracking errors for accuracy and precision ( ± standard deviation) of the instrument manipulator (IM) as tested with the vibrometer

| | **Dynamic** | | |
|---|---|---|---|
| **in µm** | **Precision (reproducibility)** | **Accuracy** | **Max Accuracy Error** |
| **Automated IM XY** | 3 ± 1 | 1 ± 1 | 39 |
| **Automated IM Z** | 2 ± 0 | >1 ± 0 | 25 |

Table 2:Inherent accuracy of the motion controller as tested using the vibrometer

| | Dynamic | | | Static | | |
|---|---|---|---|---|---|---|
| **in µm** | **Precision** (reproducibility) | **Accuracy** | **Max Accuracy Error** | **Precision** (reproducibility) | **Accuracy** | **Max Accuracy Error** |
| **XY** | 21 ± 7 | 4 ± 3 | 133 | 6 ± 5 | 4 ± 3 | 13 |
| **Z** | 29 ± 7 | 2 ± 1 | 131 | 5 ± 2 | 1 ± 0.5 | 10 |

Table 3: Average unassisted (manual) tracking errors for accuracy and precision ( ± standard deviation), viewing through a microscope

| | Dynamic | | | Static | | |
|---|---|---|---|---|---|---|
| **in µm** | **Precision** (reproducibility) | **Accuracy** | **Max Accuracy Error** | **Precision** (reproducibility) | **Accuracy** | **Max Accuracy Error** |
| **Experienced XY** | 38 ± 9 | 87 ± 6 | 555 | 25 ± 5 | 132 ± 24 | 448 |
| **Inexperience XY** | 38 ± 4 | 68 ± 6 | 365 | 31 ± 3 | 116 ± 29 | 543 |
| **Experienced Z** | 35 ± 14 | 58 ± 35 | 187 | 27 ± 8 | 52 ± 27 | 177 |
| **Inexperienced Z** | 60 ± 37 | 108 ± 79 | 389 | 36 ± 10 | 57 ± 15 | 312 |

Table 4: Average robotic assisted tracking errors for accuracy and precision ( ± standard deviation), viewing through a microscope

| | **Dynamic** | | | **Static** | | |
|---|---|---|---|---|---|---|
| **in µm** | **Precision** (reproducibility) | **Accuracy** | **Max Accuracy Error** | **Precision** (reproducibility) | **Accuracy** | **Max Accuracy Error** |
| **Experienced XY** | 24 ± 2 | 42 ± 8 | 180 | 7 ± 2 | 68 ± 24 | 146 |
| **Inexperienced XY** | 18 ± 2 | 29 ± 8 | 120 | 6 ± 1 | 39 ± 3 | 125 |
| **Experienced Z** | 32 ± 14 | 35 ± 15 | 161 | 1 ± 0 | 2 ± 1 | 11 |
| **Inexperienced Z** | 28 ± 21 | 46 ± 33 | 170 | 3 ± 2 | 3 ± 3 | 36 |

Table 5: Average tracking errors for accuracy and precision using the laser vibrometer with or without robotic assistance ( ± standard deviation), while viewing a monitor

| | | Dynamic | | | Static | | |
|---|---|---|---|---|---|---|---|
| in µm | | Precision (reproducibility) | Accuracy | Max Accuracy Error | Precision (reproducibility) | Accuracy | Max Accuracy Error |
| **Experienced horizontal** | **Assisted** | 26 ± 11 | 6 ± 4 | 246 | 9 ± 7 | 4 ± 4 | 56 |
| | **Unassisted** | 72 ± 25 | 16 ± 16 | 719 | 50 ± 20 | 7 ± 6 | 549 |
| **Inexperienced horizontal** | **Assisted** | 17 ± 8 | 3 ± 4 | 242 | 8 ± 4 | 5 ± 5 | 46 |
| | **Unassisted** | 58 ± 31 | 8 ± 7 | 963 | 44 ± 21 | 4 ± 4 | 469 |
| **Experienced vertical** | **Assisted** | 45 ± 5 | 8 ± 4 | 201 | 6 ± 3 | 3 ± 2 | 48 |
| | **Unassisted** | 48 ± 16 | 11 ± 8 | 625 | 34 ± 8 | 12 ± 9 | 206 |
| **Inexperienced vertical** | **Assisted** | 21 ± 3 | 2 ± 1 | 100 | 9 ± 4 | 7 ± 3 | 46 |
| | **Unassisted** | 54 ± 9 | 17 ± 13 | 567 | 59 ± 9 | 27 ± 7 | 543 |